Journal of
Materials Sciences and Applications

Research Article Open Access

Corrosion Susceptibility and Resistance of API 5L Steel Pipes at Seam Weld by Electrical Resistance

Pedro López-Fajardo[1], Jesús-Gilberto Godínez-Salcedo[1], Jorge-Luis González-Velázquez[1], Enrique Curiel Reyna[2], Alberto Lara-Guevara[3] and Ignacio Rojas-Rodríguez[4]

[1]Department of Metallurgic Engineering, ESIQIE-IPN, D. F. 07738, México

[2]Facultad de Estudios Superiores-Cuautitlán, Universidad Nacional Autónoma de México, Cuautitlán-Izcalli, C.P. 54740. Edo, México

[3]División de Posgrado, Facultad de Informática, Universidad Autónoma de Querétaro, Ave. de las Ciencias S/N, C.P. 76230. Querétaro, Qro. México,

[4]División Industrial, Universidad Tecnológica de Querétaro, Av. Pie de la Cuesta 2501. C.P. 76148. Querétaro, Qro. México

[*]**Corresponding author:** Rojas-Rodriguez Ignacio, División Industrial, Universidad Tecnológica de Querétaro, Av. Pie de la Cuesta 2501. C.P. 76148. Querétaro, Qro. México, Tel: + (52) 5519110779, E-mail: irojasmx@yahoo.com.mx

Received Date: October 04, 2022 **Accepted Date:** November 04, 2022 **Published Date:** November 07, 2022

Citation: Pedro López-Fajardo, Jesús-Gilberto Godínez-Salcedo, Jorge-Luis González-Velázquez, Enrique Curiel Reyna, Alberto Lara-Guevara, Ignacio Rojas-Rodríguez (2022) Corrosion Susceptibility and Resistance of API 5L Steel Pipes at Seam Weld by Electrical Resistance. J Mater sci Appl 6: 1-11

Abstract

The corrosion resistance of API 5L X70 (UNS J02500) steel pipes at seams welded by electrical resistance was evaluated by means of polarization resistance. The testing procedure was conducted according to ASTM G59-97(2009) [1]. Tests were practiced on the internal surface of API 5L X70 steel pipes. Test solutions were acid brine and brine containing H_2S prepared according to NACE 1D 182 [2]. Results showed that the seam welded by electrical resistance corroded the non-annealed pipe 27% faster than the base metal using the H_2S solution, while 16% faster than the base metal using the acid brine solution. The susceptibility of the non-annealed pipe that produced selective corrosion was studied using a 1 cm^2 sample by the stepped potential potentiostatic electrochemical test method. Tests were designed to identify predicting susceptibility methods of selective corrosion in electrical resistance welded pipes. A metallographic section of the seam pipe wall showed that the corrosion begins at the fusion line of the inside pipe surface. The study was completed with metallographic and chemical sample characterization.

Keywords: ERW Corrosion; Pipeline Steel; Pipe Seam Corrosion; Stepped Potential Potentiostatic; Electrochemical Test

Introduction

According to several authors, the excellent corrosion resistance of stainless steel in many aqueous solution results from its ability to protect itself from the corrosive environment via formation of a thin passive film [3-4] which consists of a mixture of iron and chromium oxides, with the hydroxide and water-containing compounds located at the outermost region of the passive film while the chromium oxide enrichment is found at the metal/film interface [5]. This film varies in composition from alloy to alloy and also temperature dependent. For all stainless steel, this film is stabilized by chromium oxide and it is considered nonporous, inso-luble, passive and self-healing when attacked [6]. Under conditions favorable to passivity, stainless steel has so-lution potentials approaching those of noble metals [7].

Electrical resistance welded (ERW) pipes have been widely applied, including oil and gas industries. Nevertheless, certain of these pipes have failed in operation [8-10], particularly by selective corrosion in the area of the seam weld as shown in Figure 1 [11], causing serious doubts about the reliability of this pipe type [12]. In Mexico, [1]the number of failures directly attributed to corrosion of the ERW seam has been constantly increasing in recent years, particularly in pipelines with water settlement in the stream [11]. Therefore, although there have been various studies to improve the understanding of the corrosion susceptibility of seam welds in ERW pipes [13-17], it is still necessary to have tools that facilitate monitoring the problem, as well as understanding its mechanisms and the effects of metallurgical variables on this corrosion behavior [18-20].

For these purposes, the research was designed and conducted to take advantage of the characteristics of the linear Polarization Resistance (PR) technique. This technique allows isolating specific zones of a surface such as the corrosion behavior of the seam weld, which is several millimeters wide, can be evaluated and compared to the behavior of the base metal in a series of test solutions that simulate the different electrochemical characteristics of the condensed water inside of gas and oil pipelines. On the other hand, the mechanism of grooving corrosion is believed to be a special case of pitting corrosion [15-17]. The initiation of damage is galvanically driven by the segregation of manganese sulfides, and the associated sulfur-enriched steel matrix around the sulfides, to the weld seam. An accepted method to evaluate the susceptibility of a material to pitting corrosion, or other autocatalytic localized corrosion mechanisms, is through the use of Stepped Potential Potentiostatic (SPP) electrochemical test. In this technique, the working electrode is polarized to a constant electrode potential then the current required to maintain the level of polarization is monitored as a function of time. If localized corrosion begins, an increase in the current required to maintain a given level of polarization is observed. This outcome indicates that the material is susceptible to selective corrosion.

In the pipeline industry at present, there are no effective means for predicting the susceptibility of ERW pipe to selective corrosion prior to placing them in service [21]. For these purposes, this research was designed to take advantage of the electrochemical technique like SPP to have an accelerated screening of susceptibility to selective corrosion of ERW pipe.

Figure 1: ERW pipe failed in service due to selective corrosion at the seam weld

Materials and Methods

Material and Sample Preparation

Pipes with 610 mm (24") diameter and 11.43 mm (0.45") thickness were studied. ERW pipe material was API 5L X70 (UNS J02500) steel. One of them corresponded to a pipe failed in service.

Nine samples of each pipe were cut to carry out the analysis on the cross section: three 10 mm x 10 mm x 10 mm samples were identified as base metal; three 20 mm x 10 mm x 10 mm samples that contained the failed seam weld were designated as ERW seam (Figure 2); the last three 10 mm x 10 mm x 10 mm samples from the welded section and base metal at the center were identified as welded area. Nine more samples were obtained from an ERW pipe that did not fail in service to compare against specimens of the failed pipe.

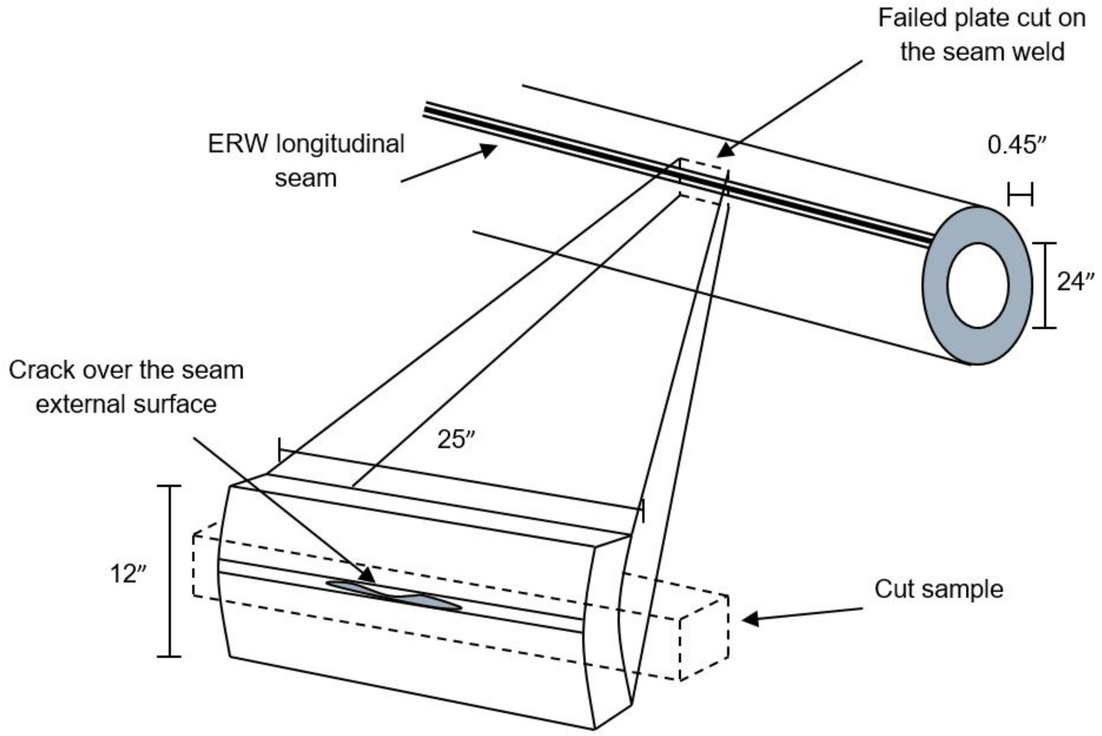

Figure 2: Diagram of the of the sample section

Metallographic and Hardness Analysis

Samples were prepared for metallographic examination following standard practices, grounded with 240, 320, 400, 600, and 1500 grit sandpapers, and then, these were polished with 0.3 mm alumina and etched with 2% Nital for 30 s. Sample microstructure was revealed according to NACE TMO 169-2000 [22] and observed by an optical microscope Olimpus. The quantification of the metallographic constituents and grain-size measurements were performed using a NIKON Ediphoto 670243 series image analyzer; according to the ASTM E45-13 [23] and ASTM E1382-97(2010) [24] procedures, respectively. Vickers micro-hardness (200gf, 12s) measurements were taken with a Future Tech series FM7249 micro indenter at weld and base metal zones of the pipe internal surface according to procedure ASTM E-140-12 [25].

Electrochemical Test

A SPP electrochemical test method was used to evaluate the susceptibility of the ERW pipe to selective corrosion. Work electrodes were taken from internal surfaces of annealed and non-annealed pipes. The work electrode was assembled in the electrochemical cell and polarized at a constant electrochemical potential (-0.3 V) above the open circuit potential. The current required to maintain the polarization level was monitored for 3.3 h.

Two solutions were used for electrochemical tests, both according to ID182 NACE standard. The first solution (brine) was a mix with 106.58 g NaCl; 4.48 g $CaCl_2.2H_2O$; 2.06 g $MgCl_2.6H_2O$; 2 ml of 2% HCl as well as distilled water to 1 liter of solution. The PH was adjusted to 3.0, and this solution was identified as “acid”. The second solution was a mix of 106.58 g NaCl; 4.48 g $CaCl_2.2H_2O$; 2.06 g $MgCl_2.6H_2O$; 3.89 g $Na_2S.9H_2O$ and 1.87 g CH_3COOH; the pH was adjusted to 5.0 with acetic acid. This solution produced an equivalent partial pressure of hydrogen sulfide (H_2S) of 40000 Pa to simulate a sour environment and was designated as “sour”.

The potentiostatic was verified according to ASTM G59; ±20 mV linear polarization scans vs open circuit potential was performed at 0.166 mV/s scan rate; five tests were practiced to obtain representative results. A saturated calomel electrode with potassium chloride (KCl) was used as reference. Scanning polarization parameters are shown in Table 1.

Table 1: Polarization parameters

Potential E_0	-0.020 V vs open circuit potential
Potential E_1	0.020 V vs open circuit potential
Step height	0.100 mV
Scan rate	0.166 mV/s
Step time	0.602 s
Number of points	401

The equipment used to evaluate material in a corrosive medium was a Princeton EG and G applied research digital potentiostatic. This equipment has a software called Power Suite that converts data obtained in potentiodynamic polarization curves. Figure 3 shows the equipment used in the laboratory tests.

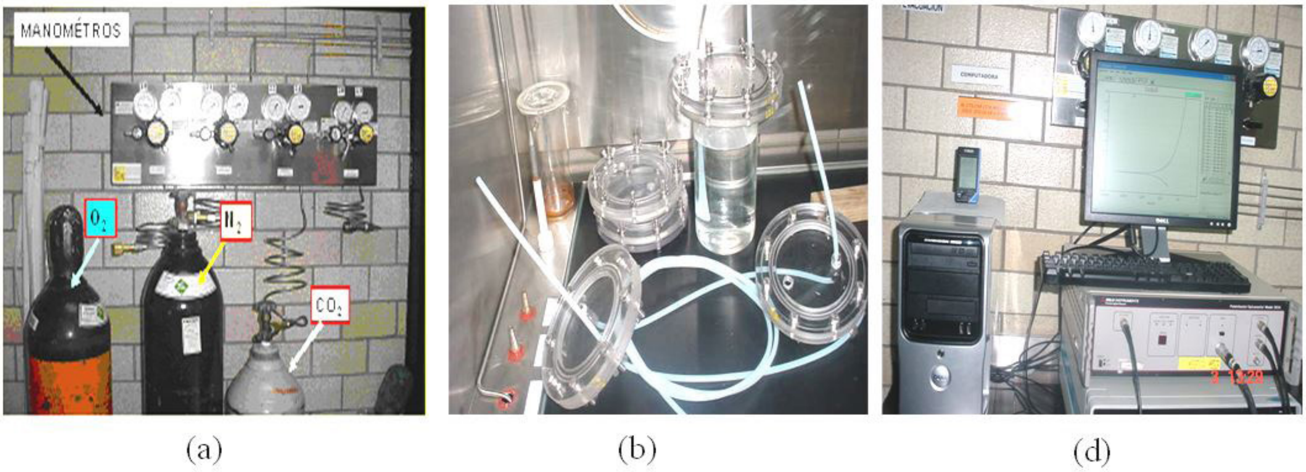

Figure 3: Princeton EG and G applied research digital potentiostatic. (a) Gases system. (b) Cell used. (c) Computer system

Results

Chemical Analysis

Chemical analysis results of the samples are given in Table 2 according to limits specified by API 5L 2000 standard

Metallographic Examination

The metallurgical microstructure evaluation was carried out at the ERW seam area. Sample microstructures were first analyzed at the base metal and at the ERW seam of the non- annealed tube condition sample. The microstructure was ferrite and pearlite with ASTM 8 grain size, as shown in Figure 4. The base metal shows in Figure 4(a) ferrite and pearlite ware homogenously distributed. The welded area shows in Figure 4(b) a microstructure with fine ferrite and pearlite uniformly distributed. The Heat Affected Zone (HAZ) shows in Figure 4(c) a microstructure with fine ferrite and pearlite but not uniformly distributed.

Table 2: Chemical analysis results (% W)

Sample	% C	% P	% S	% Mn	% Si	% Cu
Annealed	0.2	0.03	0.031	1.16	0.06	0.054
Non- annealed	0.2	0.02	0.028	0.88	0.02	0.05
API5L2000	0.18-0.23	0.03 max	0.031 max.	1.40	-	-

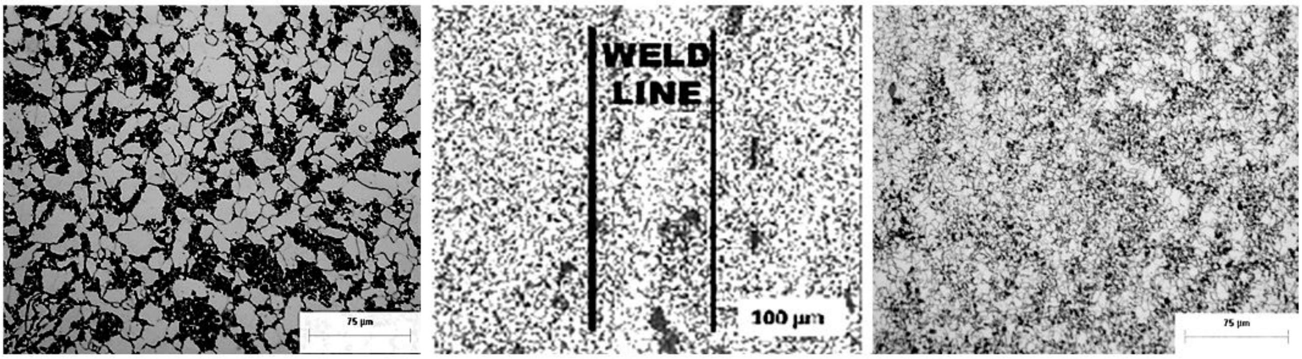

(a) (b) (c)

Figure 4: Non-annealed pipe microstructure, etched with 3% Nital [26, 27]. (a) Base metal; (b) Welded area; (c) HAZ

The second metallographic analysis was performed at the base metal and at the ERW seam area of the annealed pipe condition, as shown in Figure 5. The metallurgical structure was ferrite and pearlite, mainly with ASTM 10 grain size, were uniformly distributed. Non-metallic inclusions were mostly type II (along grain boundaries) manganese sulfides [26]. A slightly decarburized zone is observed at the weld seam with an ASTM 11 grain size. The base metal shows in Figure 5(a) ferrite and pearlite are homogenously distributed. Figure 4(b) shows fine ferrite and pearlite uniformly distributed at the welded area. Figure 4(c) shows fine ferrite and pearlite uniformly distributed. The uniform grain size was due to the normalization heat treatment.

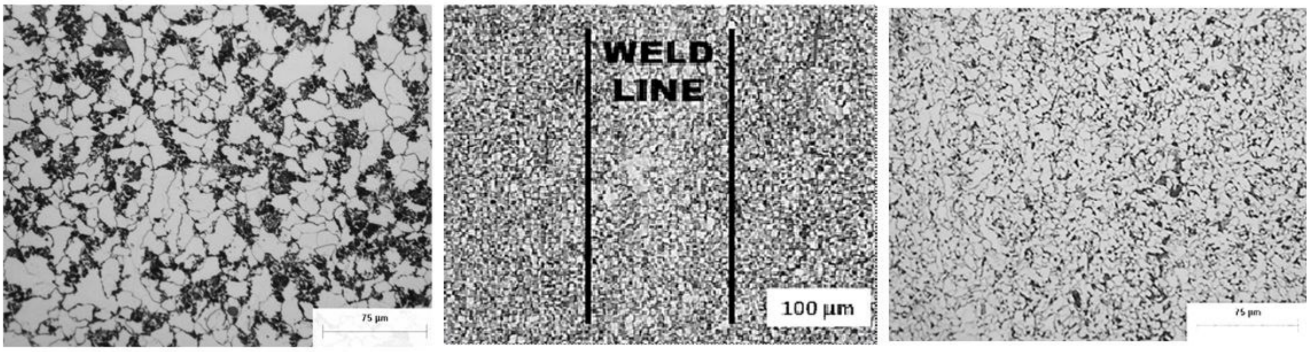

(a) (b) (c)

Figure 5: Annealed pipe microstructure, optical microscope [27]. (a) Base metal; (b) Internal surface; (c) ERW seam

Results are shown in Table 3. % Vol. ferrite and pearlite were evaluated, as well as nonmetallic inclusion, grain size and hardness.

Table 3: Quantitative microstructure features of samples

Sample/features	% vol. inclusions	% vol. ferrite	% vol. pearlite	ASTM grain size	Vickers hardness
Annealed base metal	0.45	76	24	10	187
Annealed ERW seam	0.61	68	32	11	190
Non-annealed base metal	0.62	73	27	8	214
Non-annealed ERW seam	0.80	62	38	11.5	242

Electrochemical Test

Linear PR tests

Linear PR tests were performed to determine the corrosion rate (CR) at the ERW seam weld and at the base metal in the internal surface of API5L X70 ERW steel pipes. Table 4 shows an average of five samples that were analyzed.

SPP Electrochemical Test in Acid Solution.

Figure 6 shows a microstructure comparison of the non-annealed ERW seam sample before the SPP electrochemical test in Figure 6(a) and after the test in Figure 6(b). In Figure 6(c) there is a small cavity where a slightly decarburized weld line was visible by the metallographic examination. A significative corrosion appears at the ERW seam.

Table 4: Electrochemical parameters applied in the PR tests

	Sour solution pH = 5	Acid solution pH = 3
Zone	CR [mp/y]	CR [mp/y]
Annealed base metal	23.20	36.26
Annealed ERW seam	28.15	40.10
Non-annealed base metal	23.90	29.45
Non-annealed ERW seam	30.45	34.16

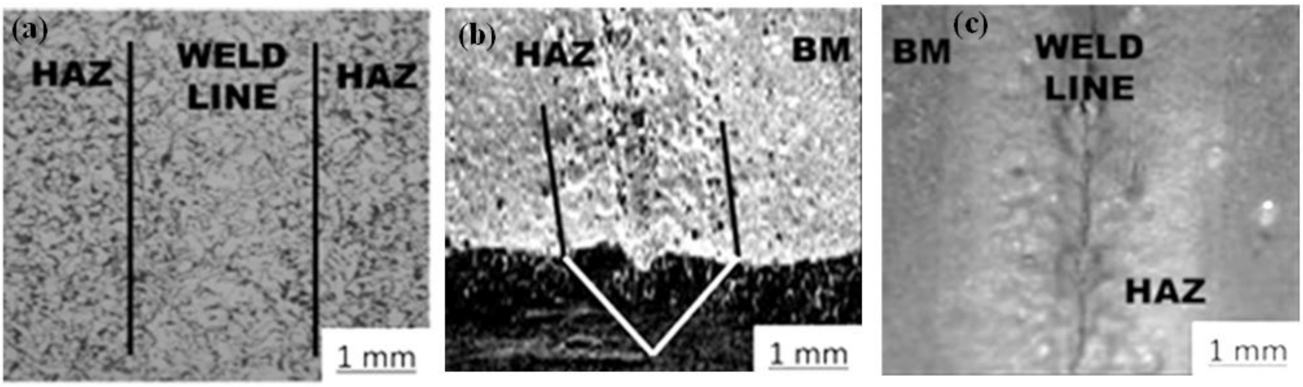

Figure 6: Internal surface microstructure of the non-annealed pipe. (a) Before corrosion test; (b) After corrosion test (c) Corrosion product

Figure 7 shows a non-annealed transverse section of ERW seam after the SPP electrochemical test. As observed, the corrosion begins at the fusion line on the pipe inside surface; the groove width corresponds to the area of coarse grained at the HAZ. The corrosion sensitivity coefficient at the groove, □, is defined [16] as: □ = h_2/h_1, where h_2 is the depth from origin surface to corrosion groove base; h_1 is the base metal corrosion depth. The grooving corrosion sensitivity coefficient average □ of non-annealed samples was 1.52, while annealed samples had 1.03.

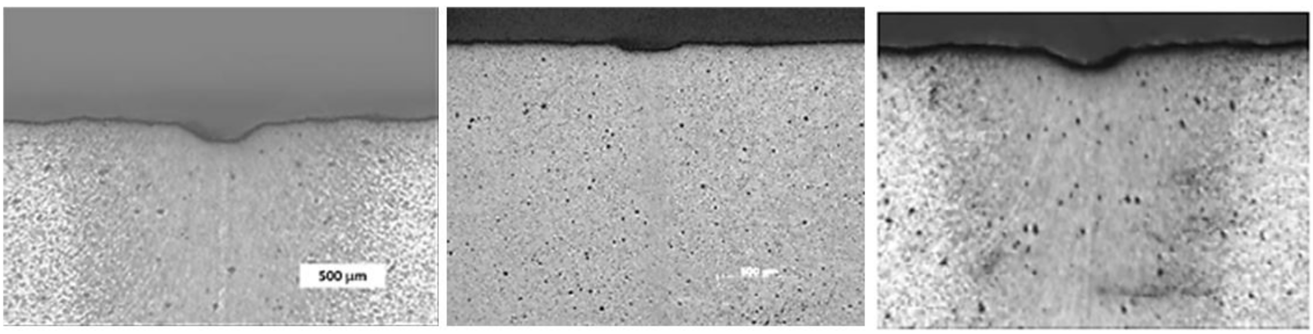

(a) (b) (c)

Figure 7: Sample wall microstructure at the ERW seam after the SPP electrochemical test.

Figure 8 shows a trend of current intensity in SPP electrochemical test. There is no significant current difference to maintain the level of polarization between the base metal and the annealed sample, except at the beginning, what can be associated with the sample damage. However, the non-annealed sample holds a significant current difference.

Figure 9 shows current intensity behavior of samples during the SPP electrochemical test in sour solution. The base metal sample increases the current until it reaches a steady value, which can be related to uniform sample corrosion. The annealed sample shows a significant drop over time, and some variation, but they could not be attributable to selective corrosion in the sample because the sample visual inspections did not show a significant damage. Finally, the non-annealed sample presented a gradual increase, reaching a peak and then decreasing to a plateau which is approximately equivalent to the base metal; this variation can be associated to a selective corrosion similar as shown in Figure 4.

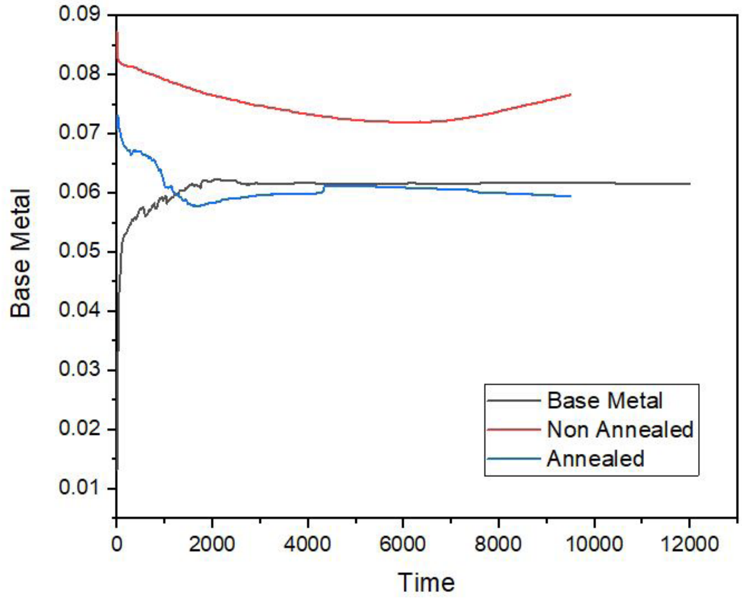

Figure 8: Current trend during 3.3 h SPP electrochemical test, corrosion test solution pH = 3

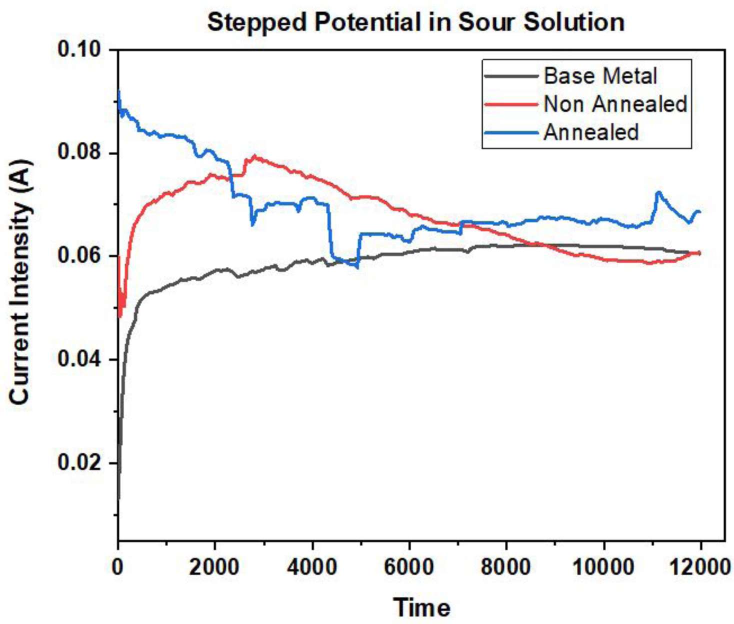

Figure 9: Current trend during 3.3 h SPP electrochemical test, corrosion test solution pH = 5

Discussion

The aim of this study (was) to assess and compare the corrosion susceptibility of ERW seam and base metal on the internal surface of API 5L X70 steel pipes. The study was conducted by means of PR tests in acid and in sour brines, which simulated the environment generated when the water condenses inside the pipeline. Results showed that the corrosion rates of the ERW seam are always higher than those of the base metal, even though the difference is not as large as those observed in in-service failures (Figure 1). For example, the highest difference observed in the PR tests was approximately 27% (non-annealed sample in sour solution). Furthermore, the differences in corrosion rate between the base metal and the ERW seam are a little greater in the sour solution, even though the corrosion rates are higher in the acid solution.

The different corrosion behavior between the ERW seam and the base metal studied can be attributed to microstructure differences. The base metal sample has a microstructure of equiaxial ferrite grains with pearlite, while the ERW seam sample has a microstructure consisting of a fine carbide dispersed in a ferrite matrix, as a result of the ERW. The most straightforward explanation is that the ERW microstructure is simply more active because it has more internal energy than the base metal. It was reported [15] that generally, localized and general corrosion rates vary slightly between different carbon steels, but the microstructure affects corrosion. Steel with coarse ferrite microstructure performs better in terms of average corrosion and the ferrite microstructure shows the lowest corrosion rate. It was deduced [15] that the metal at the fusion line should corrode faster than other metal and it is difficult to explain the grooving corrosion at the fusion line by these effects of the microstructure.

However, the former explanation is not enough to justify corrosion rates of ERW seam observed in service, which may reach values of the order of hundreds of mp/y (as in cases similar to that shown in Figure 1). Microstructural differences do not explain different corrosion rates between the base metal and the ERW seam. Corrosion rates of the base metal measured in this work are indeed similar to those observed in service [6]. In contrast, corrosion rates of the ERW seam are lower than those observed in the field [6]. The relatively lower corrosion rates of the ERW seam, as well as the smaller differences between these rates and the corrosion rates observed in the base metal, are an indication of the selective corrosion of the ERW seam, with its most extreme form of damage. Corrosion rate differences of the ERW seam observed in service might be the result of combination of the base metal and the ERW zone and not to the isolated electrochemical characteristic of these two zones.

A SPP electrochemical test was used in this work to evaluate the susceptibility of non-annealed ERW pipe to selective corrosion. The level of polarization was constant, measuring -0.3 V above the open circuit potential during 3.3 h. Visual inspection after testing revealed that the exposed sample area has experienced significant wall thinning by general corrosion, and a grooving was observed in the sample. The experimentation was called stepped potentiostatic because initially had considered carrying increments the potential if it was not possible to observe damage in the samples; however, the potential of 0.3 mV distinguished the susceptible sample. On the other hand, the potential of 0.3 mV was selected taking into account Tafel curves of samples. Metallographic examination showed that the groove at the sample is centered on the weld seam. The groove width appears to correspond to the width of the coarse-grained region of the HAZ and the difference in shallow grooving corrosion was greater in non-annealed pipes. The grooving corrosion sensitivity coefficient [16] presented a similar result and confirmed that heat treatments can effectively decrease the sensitivity to grooving corrosion. The present study has an answer to that material is more susceptible to selective corrosion, this with a lower potential (-300 mV) and less time (3.3 h). Results were reported [16] with -550 mV vs potential. Calomed saturated electrode (SCE) and polarized for 144 h. [17] Reported that grooving corrosion sensitivity coefficient decreases when steel carbon content decreases. Samples had the same carbon content in this study so that the coefficient variation is attributed only to different heat treatment. Maricica Stoica et al. carried out a similar study, but in solutions consisting of biocide (Oxonia-Active®) and Aspergillus niger suspension, where they found that bio OA is more destructive to AISI 316L stainless steel [28].

Conclusions

Results showed that

1) The ERW seam in the non-normalized pipe corrodes 27% faster than the base metal in the H_2S solution and 16% in the acid brine solution.

2) The ERW seam weld in the normalized tube corrodes 21% and 11% faster than the base metal in the H_2S and acid brine solutions.

3) The differences in corrosion rates are greater in non-normalized pipes tested in the H_2S solution. However, the corrosion rates are larger in acid brine.

4) By the SPP electrochemical test, the sample showed a small cavity in the place at which the slightly decarburized weld line was visible with the metallographic examination.

5) It is evident that the corrosion was higher at the ERW seam.

Summary

The PR test of the isolated ERW seam and base metal zones in API 5L X70 steel pipe show that the ERW seam zone is corroded faster than the base metal with greater differences in corrosion rate in the sour solution. Even though the acid solution gave the highest corrosion rates. The electrochemical behavior in both cases was active with a mechanism of aqueous dissolution. Corrosion behavior differences between the two zones were, at first, attributed to microstructure differences between the base metal and the ERW seam; however, this difference is not enough to explain the greater differences observed in service, which indicates that other factors may play an important role in defining the overall corrosion rates, such as the combined behavior of the base metal and the weld zone or an unfavorable area ratio. Conversely, the SPP electrochemical test could be a promising technique to accelerate ERW weld screening susceptible to selective corrosion because testing has allowed a corrosion level differentiation in a short time.

Conflicts of Interest

The authors declare no conflicts of interest regarding the publication of this paper.

References

1. ASTM G59-97 (2009) Standard Test Method for Conducting Potentiodynamic Polarization Resistance Measurements.

2. NACE Technical Publication 1D.182. (2005) Wheel Test Method Used for Evaluation of Film-Persistent Corrosion Inhibitors for Oilfield Applications. NACE International.

3. Gasparac R, Martin C (2001) Investigations of the Mechanism of Corrosion Inhibition by Polyaniline. Polyaniline-Coated Stainless Steel in Sulfuric Acid Solution. Journal of The Electrochemical Society 148: 4-11.

4. Callister Jr WD (2003) Materials Science and Engineering an Introduction. 6th Edition, John Wiley &Sons, lnc., Hoboken

5. Loto CA, Mohammed AI (2005) Corrosion Resistance and Susceptibility of Type 304 Stainless Steels in Strong Acids. NSE Tech Trans 40: 88-106.

6. United States Environmental Protection Agency (2001) Report on the Corrosion of Certain Alloys. United States Environmental Protection Agency, Washington DC.

7. Kruger J (2000) Basics of Corrosion Science and Engineering. McGraw-Hill, New York.

8. Kiefner JF (1992) ERW Line Pipe, Installed Pipe, especially pre-1970, plagued by Problems, Oil & Gas Journal 90: 32.

9. Masamura K, Matsushima I (1981) Grooving Corrosion of Electric Resistance Welded Steel pipe in Water- Case Histories and Effects of Alloying Elements; Presented at Corrosion '81, NACE International 75.

10. MacNab AJ (2003) Observations of Corrosion of Eelectric Resistance Welded Galvanized Steel Pipe in Domestic Potable Water, Corrosion 03269.

11. Polytechnic National Institute (IPN) (2010) Field Reports of Equipment in Service of Petroleum Mexicans (PEMEX). Group of Analysis of Integrity of Ducts (GAID).

12. National Academies (2004) Transmission Pipelines and Land Use: A Risk-Informed Approach Special Report 281. Transportation Research Board (TRB) Washington, D.C.

13. Duran C, Treiss E, Hebsleb G (1986) The Resistence of High Frecuency Inductive Welded Pipe to Grooving Corrosion in Salt Water. Materials Performance 25: 41-8.

14. Kato C, Otoguro Y, Kado S, Hisimatsu Y (1978) Grooving Corrosion in Electric Resistance Welded Steel Pipe in Sea Water. Corrosion Science 18: 61-74.

15. Lukezich SJ (1998) Susceptibility of Modern ERW Pipe to Selective Weld Seam Corrosion in Wet Environments. Technology for Energy Pipelines. Catalog No. L51775e. Pipeline Research Council International, PR15-9306, United States.

16. Bi Z, Wang R, Jing X (2012) Grooving Corrosion of Oil Coiled Tubes Manufactured by Electrical Resistance Welding. Corros. Sci 57: 67-73.

17. Wang R, Luo S (2013) Grooving Corrosion of Electric-Resistance-Welded Oil Well Casing of J55 steel. Corros. Sci 68: 19-127.

18. Lee B, Lee S (2004) Studies on the Microestructure and Corrosion Characteristics of Electrical Resistance Welded Steel. Key Engineering Materials, III: 2327-31.

19. Guo J, Yang SW, Shang CJ, Wang Y, He XL (2008) Influence of Carbon Content and Microstructure on Corrosion Behaviour of Low Alloy Steels in a Cl- Containing Environment. Corros. Sci 51: 242-51.

20. Nakata H, Kami C, Nobuyuki M (2008) Development of API X-80 Grade Electric Resistance Welding Line Pipe with Excellent low Temperature Toughness, JFE Technical Report 12: 27-31.

21. Meade R (2006) Non-Destructive Evaluation of Low-frequency Electric Resistance Welded (ERW) Pipe Utilizing Ultrasonic In-Line Inspection Technology. Tuboscope Pipeline Services, Houston, Texas.

22. NACE TM0169 (2000) Standard Test Method-Laboratory Corrosion Testing of Metals.

23. ASTM E45-13 (2018) Standard Test Methods for Determining the Inclusion Content of Steel.

24. ASTM E1382-97 (2010) Standard Test Methods for Determining Average Grain Size Using Semiautomatic and Automatic Image Analysis.

25. ASTM E140-12be1. (2019) Standard Hardness Conversión Tables for Metals Relationship Among. Brinell Harness, Vickers Hardness. Rockwell Hardness, Superficial hardness, Knoop Hardness, Scleroscope Hardness, and Leeb Hardness.

26. Murty YV, Kattamis TZ, Mehrabian R, Flemings MC (1977) Behavior of Sulfide Inclusions during Thermomechanical Processing of AISI 4340 Steel. Metallurgical Transactions A 8: 1275-82.

27. Reagents Nital 3% (2016) MSDS, According to Regulation (EC) No 1907/2006.

28. Maricica Stoica, Lina Mikoliūnaitė, Almira Ramanavičienė, Petru Alexe, Geta Carac, Rodica Dinica, Jaroslav Voronovič, Arūnas Ramanavičius. Corrosion study of stainless steel incubated in solutions consisting of biocide (Oxonia- Active®) and Aspergillus niger suspension. Chemija. 2012. 23: 180-6